Convergence Characteristics and Wielandt Acceleration of the Time Source Method for Monte Carlo Alpha Eigenvalue Calculations

Toshihiro Yamamoto[a*], Hiroki Sakamoto[b]

[a]*Institute for Integrated Radiation and Nuclear Science, Kyoto University, 2 Asashiro Nishi, Kumatori-cho, Sennan-gun, Osaka, 590-0494, Japan*
[b]*Radiation Dose Analysis and Evaluation Network, 4-13-14, Kokubunji-shi, Tokyo, 185-0001, Japan*

Abstract

This paper discusses the source convergence of Monte Carlo calculations for α-eigenvalues. Compared with the conventional "k–α method", the "time-source method" has a strong neutronic coupling even in a system where the fission sources are loosely coupled. The dominance ratio of the time source is smaller than that of the k–α method. The time-source method has a drawback in that it requires a much longer computation time. Furthermore, the time-source method cannot be applied to critical or supercritical systems owing to the long fission chain. A new technique is developed to overcome these drawbacks by introducing the Wielandt method for increasing the dominance ratio. This technique, which uses the Wielandt method in an opposite manner, reduces the computation time and expands the availability in a supercritical system. Because the source convergence of the time-source method is inherently stable, the new method causes a limited adverse effect on the source convergence.

Keywords: alpha-eigenvalue; Monte Carlo; fission source; convergence; Wielandt acceleration

1. Introduction

There are mainly two kinds of eigenvalue modes in the eigenvalue problem of neutron transport in a multiplying system: k_{eff}-eigenvalue mode and α-eigenvalue mode. In the equation for k_{eff}-eigenvalue, the fission operator is divided by k_{eff}-eigenvalue. On the other hand, the α-eigenvalue is a decay or growth constant of neutron population that exponentially decays or

* Corresponding author. Tel:+81 72 451 2414
E-mail address: toshihiro.yamamoto223@gmail.com (T. Yamamoto)

grows with time, respectively. The equation for k_{eff}-eigenvalue can be transformed to the equation for α-eigenvalue by adding a term $\alpha\phi/v$ and setting $k_{eff} = 1$ where v is the neutron speed and ϕ is the neutron flux. The conventional Monte Carlo α-eigenvalue (prompt neutron time decay constant) calculation method is based on the utilization of the fission source power iteration method for k_{eff}-eigenvalue calculations (Brockway et al., 1985; Yamamoto and Miyoshi, 2003; Yamamoto, 2011; Zoia et al., 2014, Kiedrowski, 2014). The α-eigenvalue is iteratively updated at the end of each power iteration generation such that the ratio of the fission neutrons between the successive generations approaches unity. This method has been known as the k–α method. The k–α method is known for its drawback of instability in deeply subcritical systems owing to excessive neutrons produced by the large α-eigenvalue. A different approach for the Monte Carlo α-eigenvalue calculation, i.e., the "time-source method," has been proposed by Shim et al. (2014, 2015) and Josey and Brown (2019). Whereas the fission source is generated by fission reaction, the time source is defined by the product of the neutron flux and $1/v$, where v is the neutron speed. The α-eigenvalue that is sought in the time-source method is an eigenvalue of the α-mode eigenvalue equation, whereas the α-eigenvalue in the k–α method is sought as an adjustment parameter to obtain a ratio of the fission neutrons between the successive cycles.

The time-source method is suitable for the sensitivity analysis of the α-eigenvalue because the sensitivity coefficients of the α-eigenvalue to nuclear data can be obtained with the differential operator sampling (DOS) method in the same manner that the DOS method was used for calculating the sensitivity coefficients of the k_{eff}-eigenvalue (Yamamoto, 2018). Previously, the authors of this paper proposed a sensitivity analysis method of the α-eigenvalue based on the time-source method (Yamamoto and Sakamoto, 2019a; Yamamoto and Sakamoto, 2019b). It is challenging to use the time-source method for a system containing a void region where no collision occurs because no time source can be generated. This difficulty can be avoided by allocating a pseudo scattering material in the void region, which is similar to the delta tracking technique (Yamamoto and Sakamoto, 2019a; Woodcock, 1965).

In the time-source method, fission neutrons and all their progenies must be tracked within a cycle until they are exterminated by leakage or the Russian roulette. The "cycle" in the time source method begins with the emission of the neutrons from the time source and ends with the annihilation of the all progenies of the source neutrons over multiple generations. Therefore, as the system approaches the prompt criticality, the fission chain extends over more generations, thereby significantly prolonging the computation time for one cycle. If the system exceeds the prompt criticality, the fission chain lasts infinitely, and the time-source method is no longer applicable. One of the objectives of this study is to propose a new method to circumvent the problem of the long or endless fission chains, thereby expanding the availability of the time-source method.

Another objective of this study is to investigate the source convergence in α-eigenvalue calculations. The problem of fission source convergence in k_{eff}-eigenvalue Monte Carlo calculations has garnered attention for decades. Many papers have been published regarding the diagnosis and acceleration methods of fission source convergence. In particular, slow and unstable fission source convergence has occurred in a loosely coupled fissile array (Whitesides, 1971; Yamamoto et al., 2000; Brown, 2011; Ueki, 2012), which is known as the "*k*-effective of the world" problem. The fission source convergence in the k–α method is considered to be similar to k_{eff}-eigenvalue calculations because the convergence in the k–α method is dominated by the fission source distribution. Meanwhile, a different phenomenon is expected in the source convergence of the time-source method. This is because time sources are generated even in a neutron isolator made of a non-fissile material (including void) that prevents neutronic coupling between fissile arrays. Herein, the source convergence of the k–α and time-source methods are examined in addition to the proposal of acceleration in the time-source method.

The development of the α-eigenvalue calculations, which includes the asymptotic behavior of the delayed neutrons, have been performed in recent years (Nauchi, 2014; Zoia et al., 2015; Josey and Brown, 2018; Nauchi, 2019; Vitali et al., 2020). The α-eigenvalue calculations in which the asymptotic behavior of the delayed neutrons is considered must solve a nonlinear

neutron transport equation. The scope of this study is limited to addressing a situation where delayed neutrons are neglected and only prompt fission neutrons are considered.

2. Review of Monte Carlo α-eigenvalue calculation methods

This section briefly reviews a few representative Monte Carlo α-eigenvalue calculation methods. Therefore, some contents of this section may be a duplication of previous studies, such as (Yamamoto and Miyoshi, 2003; Yamamoto, 2011; Yamamoto and Sakamoto, 2019a).

2.1 k-α method

First, the k–α method is presented. The α-eigenvalue mode neutron transport equation is as follows:

$$\boldsymbol{L}\phi(\boldsymbol{r},\boldsymbol{\Omega},E)+\frac{\alpha}{v(E)}\phi(\boldsymbol{r},\boldsymbol{\Omega},E)\ =\frac{1}{k_p}\boldsymbol{F}\phi(\boldsymbol{r},\boldsymbol{\Omega},E), \tag{1}$$

where

$$\boldsymbol{L}\phi(\boldsymbol{r},\boldsymbol{\Omega},E)=\boldsymbol{\Omega}\cdot\nabla\phi(\boldsymbol{r},\boldsymbol{\Omega},E)+\Sigma_t(\boldsymbol{r},E)\phi(\boldsymbol{r},\boldsymbol{\Omega},E)$$
$$-\int_{4\pi}d\boldsymbol{\Omega}'\int dE'\Sigma_s(\boldsymbol{r},\boldsymbol{\Omega}'\rightarrow\boldsymbol{\Omega},E'\rightarrow E)\phi(\boldsymbol{r},\boldsymbol{\Omega}',E'), \tag{2}$$

$$\boldsymbol{F}\phi(\boldsymbol{r},\boldsymbol{\Omega},E)=\frac{\chi_p(E)}{4\pi}\int_{4\pi}d\boldsymbol{\Omega}'\int dE'\nu_p\Sigma_f(\boldsymbol{r},E')\phi(\boldsymbol{r},\boldsymbol{\Omega}',E')\ , \tag{3}$$

Σ_t = the macroscopic total cross section, Σ_s = the macroscopic scattering cross section, Σ_f = the macroscopic fission cross section, χ_p = the prompt neutron spectrum, ν_p = the number of prompt neutrons per fission, and v = the neutron velocity. Because k_p in Eq. (1) is supposed to be unity in the α-eigenvalue mode calculation, α on the left-hand side is sought such that k_p becomes unity. Eq. (1) was derived by substituting the time-dependent neutron flux $\phi(\boldsymbol{r},\boldsymbol{\Omega},E,t)$ in the time-dependent neutron transport equation

$$\boldsymbol{L}\phi(\boldsymbol{r},\boldsymbol{\Omega},E,t)+\frac{1}{v(E)}\frac{\partial}{\partial t}\phi(\boldsymbol{r},\boldsymbol{\Omega},E,t)\ =\boldsymbol{F}\phi(\boldsymbol{r},\boldsymbol{\Omega},E,t), \tag{4}$$

with $\phi(\boldsymbol{r},\boldsymbol{\Omega},E)exp\ (\alpha t)$ and dividing the resulting equation by $exp\ (\alpha t)$. Eq. (1) is similar to the eigenvalue equation for k_{eff} except that the second term on the left-hand side, $\alpha/v(E)\cdot\phi(\boldsymbol{r},\boldsymbol{\Omega},E)$, exists and that the delayed neutrons are neglected. The power iteration algorithm for k_{eff}-eigenvalue calculations can be used to calculate k_p in Eq. (1). Unlike the k_{eff}-eigenvalue calculation, we must consider the second term on the left-hand side of Eq. (1). Hence, each time

the particle travels a distance s_j in the jth flight path, the weight W_j before the flight changes to the following:

$$W_{j+1} = W_j \cdot exp\left(\frac{-\alpha}{v_j(E)} s_j\right), \tag{5}$$

where α is determined in the previous generation. The typically adopted methods for considering the additional term, $\alpha\phi/v$, is the adjustment of cross sections (Zoia et al., 2014; Josey and Brown, 2018). Meanwhile, the method expressed as Eq. (5) can be applied without any modification even when the system contains a void region and whether α is positive or negative. At the end of each generation, k_p is calculated in the same manner as in the k_{eff}-eigenvalue calculations. The α used for Eq. (4) in the next generation is obtained such that k_p approaches unity, as follows:

$$\alpha_{m+1} = \alpha_m + b\left(k_{p,m} - 1\right), \tag{6}$$

where m is the generations index and b is a positive value. The α-eigenvalue is calculated by the arithmetic mean of α_m beyond the skipped generations. Because the latest α-eigenvalue is updated using the α-eigenvalue in the previous generation, an intergeneration correlation exists in the α-eigenvalue owing to Eq. (6) as well as the fission source distribution inherited from the previous genration. Therefore, the standard deviation of the mean α values is more underestimated than the k_{eff}-eigenvalue. The underestimation should be discussed as another topic and is out of the scope of this study.

2.2 Time-source method

The time-source method is a different approach for α-eigenvalue calculations (Shim, 2014, 2015; Yamamoto and Sakamoto, 2019a). In this section, the Monte Carlo algorithm of the time-source method is briefly explained.

The eigenvalue equation to be solved for the time-source method is the following:

$$\boldsymbol{L}\phi(\boldsymbol{r},\boldsymbol{\Omega},E) - \boldsymbol{F}\phi(\boldsymbol{r},\boldsymbol{\Omega},E) = -\frac{\alpha}{v(E)}\phi(\boldsymbol{r},\boldsymbol{\Omega},E)\,, \tag{7}$$

which is the same as Eq. (1) except that k_p is no longer necessary. The time source is defined by the right-hand side of Eq. (7). The time sources at the mth cycle, which are used for the next cycle, are sampled stochastically at each collision site during the course of the random walk

process, as follows:

$$n = \mathrm{Int}\left[|\alpha_{m-1}| \cdot \frac{w}{v(E)\Sigma_t(\boldsymbol{r}, E)} + \xi\right], \tag{8}$$

where $n =$ the number of time sources at the collision site, $w =$ the weight of the particle before collision, $\xi =$ uniform pseudo random number between 0 and 1, and $m =$ the cycle index. Int [x] denotes the largest integer less than or equal to x; α_{m-1} is the α-eigenvalue calculated in the previous cycle. By introducing α_{m-1} in Eq. (8), the number of time sources in each cycle can be almost unchanged over all the cycles. The information required for the fission source in the k–α method are the position and the nuclide that causes the fission. Meanwhile, those of the time-source method are the energy, direction, and position, which are the same as those of the colliding particle. Hence, the memory storage of the time-source method is larger than that of the k–α method. The α-eigenvalue using the collision estimator is obtained at the end of each cycle as follows:

$$\alpha_{m,c} = -\frac{S_m}{\sum_j \sum_i w_{ij} v(E_{ij})^{-1} \Sigma_t(\boldsymbol{r}_{ij}, E_{ij})^{-1}}, \tag{9}$$

where i and j denote the ith collision and jth source particles, respectively; $S_m =$ the sum of the source particle's weight in the mth cycle. The α-eigenvalue using the track length estimator is expressed as follows:

$$\alpha_{m,tr} = -\frac{S_m}{\sum_j \sum_i w_{ij} s_{ij} v(E_{ij})^{-1}}, \tag{10}$$

where i denotes the ith track, and $s_{ij} =$ the track length of the ith track from the jth source particle.

In the time-source method, fission neutrons and all their progenies that are generated by the second term on the left-hand side of Eq. (7) must be followed within the cycle; therefore, the computation time of the time-source method is longer compared with that of the k–α method. The computation time required for following the fission neutrons varies depending on the system's multiplication factor. As the prompt neutron multiplication factor, $k_{eff,p}$ approaches unity, the computation time per source particle becomes longer. If $k_{eff,p}$ is larger than unity, the time-source method is not applicable owing to the endlessly continuing fission chain. A

solution for this problem will be proposed later herein.

3. Source convergence of α-eigenvalue calculation

The dominance ratio of the fission source power iteration is the ratio of the second-largest k_{eff}-eigenvalue to the largest k_{eff}-eigenvalue. That is, the dominance ratio is defined in such a way that the convergence of flux to the fundamental mode is faster when the dominance ratio is smaller. The dominance ratio determines the speed or stability of the fission source convergence. In the k–α method, the largest eigenvalue of k_p is unity. Therefore, the dominance ratio of the k–α method can be expressed as

$$\rho_f \equiv k_{p,1}, \tag{11}$$

where $k_{p,1}$ is the first higher-order eigenvalue of k_p in the α-eigenvalue mode equation, Eq. (1). When obtaining $k_{p,1}$, the α in Eq. (1) is fixed at the fundamental mode α-eigenvalue.

The dominance ratio of the time-source method is analogously defined by

$$\rho_t \equiv \frac{\alpha_0}{\alpha_1}, \tag{12}$$

where $\alpha_0 =$ the α-eigenvalue of the fundamental mode; $\alpha_1 =$ the α-eigenvalue of the first higher-order mode. The difference of the two dominance ratios is discussed using a simple model below.

Based on the one-dimensional one-energy group diffusion theory, the fundamental mode α-eigenvalue equation is expressed as

$$DB_0^2 + \Sigma_a - \nu_p\Sigma_f + \frac{\alpha_0}{v} = 0, \tag{13}$$

where D = the diffusion coefficient; $B_0^2 =$ the geometrical buckling of the fundamental mode; $\Sigma_a =$ the absorption cross section. When the geometry is a one-dimensional slab of width H (including the extrapolated length), $B_0^2 = (\pi/H)^2$. The first higher-order mode equation of the k–α method is expressed as

$$DB_1^2 + \Sigma_a - \frac{\nu_p\Sigma_f}{k_{p,1}} + \frac{\alpha_0}{v} = 0, \tag{14}$$

where $B_1^2 = (2\pi/H)^2$ (the geometrical buckling of the first higher-order mode). Therefore, $k_{p,1}$ (i.e., the dominance ratio of the k–α method, ρ_f) is expressed as

$$\rho_f = k_{p,1} = \frac{\nu_p\Sigma_f}{DB_1^2 + \Sigma_a + \frac{\alpha_0}{v}} = \frac{\nu_p\Sigma_f}{D(B_1^2 - B_0^2) + \nu_p\Sigma_f}\ . \tag{15}$$

Meanwhile, the first higher-order mode equation of the time-source method is expressed as

$$DB_1^2 + \Sigma_a - \nu_p\Sigma_f + \frac{\alpha_1}{v} = 0. \quad (16)$$

Using Eqs. (13) and (16), the dominance ratio of the time-source method is as follows:

$$\rho_t = \frac{\alpha_0}{\alpha_1} = \frac{DB_0^2 + \Sigma_a - \nu_p\Sigma_f}{DB_1^2 + \Sigma_a - \nu_p\Sigma_f}. \quad (17)$$

The dominance ratios are obtained using the constants below:

$$D = 1 \text{ cm}, \ \Sigma_a = 0.1 \text{ cm}^{-1}, \ H = 30 \text{ cm} \ \ v = 3\times10^5 \text{ cm/s},$$

and $\nu_p\Sigma_f$ is a variable parameter. The dominance ratios ρ_f and ρ_t are compared in Fig. 1 as a function of $k_{eff,p}$ where $k_{eff,p} = \nu_p\Sigma_f/(DB_0^2 + \Sigma_a)$. Whereas ρ_t decreases with $k_{eff,p}$, ρ_f shows an inverse tendency. Because the numerator of Eq. (17) is zero for $k_{eff,p}$=1, ρ_t approaches zero as the system approaches the prompt critical state, which explains the decrease in ρ_t with $k_{eff,p}$. Fig. 1 illustrates that $\rho_f > \rho_t$ when $k_{eff,p} > 0.5$. Therefore, the convergence of the time source requires less cycles and is more stable than that of the fission source unless the system is significantly below the prompt criticality. The time-source method is robust in terms of source convergence, especially in nearly prompt critical systems. However, the lower dominance ratio does not necessarily mean better computational performance. This issue will be discussed in the numerical tests in Section 5.

[Fig. 1]

4. Wielandt method for α-eigenvalue calculation

The Wielandt method is applied to Monte Carlo k_{eff}-eigenvalue calculations to improve fission source convergence. In particular, the effect of the Wielandt method is remarkable in a system with a dominance ratio close to unity (Yamamoto and Miyoshi, 2004; Brown, 2005). Introducing the Wielandt method reduces the dominance ratio, which enables source convergence to be achieved in fewer power iterations. In this study, we attempt to apply the Wielandt method to Monte Carlo α-eigenvalue calculations that use the time-source method, although it has already been proposed for deterministic methods (Wachspress, 1966). With the analogy of the Wielandt method for the fission source power iteration method, the α-eigenvalue mode transport equation based on using the Wieland method is rewritten from Eq. (7) as follows (Wachspress, 1966):

$$\boldsymbol{L}\phi(\boldsymbol{r},\boldsymbol{\Omega},E)-\boldsymbol{F}\phi(\boldsymbol{r},\boldsymbol{\Omega},E)+\frac{\alpha_e}{v(E)}\phi(\boldsymbol{r},\boldsymbol{\Omega},E)=(-\alpha+\alpha_e)\frac{1}{v(E)}\phi(\boldsymbol{r},\boldsymbol{\Omega},E)\,, \tag{18}$$

where $\alpha_e =$ the shifted α-eigenvalue. The third term on the left-hand side of Eq. (18) can be treated in the same manner as in the k–α method. Hence, each time the particle travels a distance s_j in the jth flight path, the initial weight W_j changes as follows:

$$W_{j+1}=W_j\cdot exp\left(\frac{-\alpha_e}{v_j(E)}s_j\right). \tag{19}$$

Eq. (8), which determines the time sources in the next cycle, can be rewritten as

$$n=\mathrm{Int}\left[|-\alpha_{m-1}+\alpha_e|\cdot\frac{w}{v(E)\Sigma_t(\boldsymbol{r},E)}+\xi\right]. \tag{20}$$

The α-eigenvalue can be obtained by the collision and track length estimators, separately, as follows:

$$\alpha_{m,c}=-\frac{S_m}{\sum_j\sum_i w_{ij}v(E_{ij})^{-1}\Sigma_t(\boldsymbol{r}_{ij},E_{ij})^{-1}}+\alpha_e, \tag{21}$$

$$\alpha_{m,tr}=-\frac{S_m}{\sum_j\sum_i w_{ij}s_{ij}v(E_{ij})^{-1}}+\alpha_e. \tag{22}$$

In a k_{eff}-eigenvalue problem using the Wielandt method, the dominance ratio is expressed as (Wachspress, 1966)

$$\rho_k\equiv\frac{\frac{1}{k_{eff}}-\frac{1}{k_e}}{\frac{1}{k_{eff,1}}-\frac{1}{k_e}}, \tag{23}$$

where $k_{eff} =$ the fundamental eigenvalue of the k_{eff}-eigenvalue mode; $k_{eff,1} =$ the first higher-order eigenvalue of the k_{eff}-eigenvalue mode; $k_e =$ a parameter for the Wielandt method. The dominance ratio of the time-source method using the Wielandt method is analogously expressed as

$$\rho_t\equiv\frac{\alpha_0-\alpha_e}{\alpha_1-\alpha_e}. \tag{24}$$

In Eq. (23), k_e must be selected to be larger than k_{eff}. The Wielandt method is typically used to reduce the dominance ratio by selecting a negative value for α_e. However, a positive value can be selected for α_e. Even if α_e is a positive value, Eqs. (19) through (22) would hold. When α_e is a positive value, the weight of a particle decreases as it travels, as suggested by Eq. (19). Therefore, a positive value of α_e shortens the long fission chain in a nearly prompt critical

system and reduces the computation time for each source particle. In particular, when a prompt multiplication factor, $k_{eff,p}$, is larger than unity, the time-source method fails, as stated previously. Even in such a case, the time-source method is applicable by selecting α_e as follows:

$$\alpha_e > \alpha_0 > 0, \tag{25}$$

where α_0 is a positive value for a super prompt critical system, as defined in Section 2.1.

Because α_0 is larger than α_1, a positive value of α_e increases the dominance ratio according to Eq. (24), and the source convergence is worsened. However, as shown in Fig. 1, the dominance ratio of the time-source method is inherently low except in deeply subcritical systems. It is anticipated that the increase in the dominance ratio caused by a positive α_e value will not significantly deteriorate the source convergence. Fig. 2 shows the dominance ratio ρ_t as a function of $k_{eff,p}$ for several α_e. Even when $\alpha_e = 5000\ s^{-1}$, the dominance ratio is still smaller than 0.8, and the source convergence is considered to be stable.

[Fig. 2]

The Wielandt method for k_{eff}-eigenvalue calculations is applicable to the k–α method for improving the fission source convergence:

$$\boldsymbol{L}\phi(\boldsymbol{r},\boldsymbol{\Omega},E) + \frac{\alpha}{v(E)}\phi(\boldsymbol{r},\boldsymbol{\Omega},E) - \frac{1}{k_e}\ \boldsymbol{F}\phi(\boldsymbol{r},\boldsymbol{\Omega},E) = \left(\frac{1}{k_p} - \frac{1}{k_e}\right)\boldsymbol{F}\phi(\boldsymbol{r},\boldsymbol{\Omega},E). \tag{26}$$

Because k_p is supposed to be unity, k_e must be selected to be larger than unity. The algorithm of the Wielandt method for the k–α method is the same as that for k_{eff}-eigenvalue calculations.

In the k_{eff}-eigenvalue calculations, introducing the Wielandt method changes the expected number of fission neutrons per a history by a factor of (Shim and Kim, 2009)

$$L = 1 + \frac{k_{eff}}{k_e} + \left(\frac{k_{eff}}{k_e}\right)^2 + \cdots = \frac{1}{1 - k_{eff}/k_e}\,. \tag{27}$$

This factor L for the number of the time sources is analogously:

$$L\ = \frac{1}{1 - \alpha_e/\alpha_0}\,. \tag{28}$$

Because $\alpha_0 < 0$ in a subcritical system, selecting a positive value of α_e decreases the number of the time sources and also decreases the computational time per a history.

5. Numerical examples

5.1 Overview of test problems

Numerical examples for testing the source convergence of the time-source method for α-eigenvalue calculations are presented in this section. The calculations were performed for a one-dimensional two-slab array system, as shown in Fig. 3. The two fissile slabs were separated by an 18-cm-thick isolator made of light water. The light-water isolator was sufficiently thick such that this slab system was loosely coupled. The fissile slab comprised a homogenized light-water moderated UO_2 fuel rod array. The calculations were performed using an in-house research-purpose code and three-energy group constants, which are listed in Table 1. Isotropic scattering was assumed in this study. The geometry of the slab system was symmetric but loosely coupled owing to the thick isolator. Therefore, the reference solution of the converged source distribution was symmetric.

[Fig. 3][Table 1]

5.2 Convergence in slightly below prompt criticality

The first example addresses a system slightly below the prompt criticality, where $k_{eff,p} \approx 0.996$ and the fundamental mode α-eigenvalue $\alpha_0 \approx -102$ s^{-1}. The slab thickness W shown in Fig. 3 is 16.4 cm. The fission matrix method was used to assess the neutronic coupling quantitatively, as follows (Dufek and Gudowski, 2009; Carney et al., 2014; Pan et al., 2015; Dufek and Holst, 2016):

$$\begin{pmatrix} P_{11} & P_{21} \\ P_{12} & P_{22} \end{pmatrix} \begin{pmatrix} S_1 \\ S_2 \end{pmatrix} = k_p \begin{pmatrix} S_1 \\ S_2 \end{pmatrix}, \tag{29}$$

where the matrix element $P_{ij} =$ the probability of a fission neutron born in slab j owing to one average fission neutron starting in slab i; $S_i =$ the fission neutrons in slab i; $k_p =$ the eigenvalue of the fission matrix. Note that this fission matrix is in the α-eigenvalue mode and differs from the conventional one that is defined in the k_{eff}-eigenvalue mode. The eigenvalue of Eq. (29), k_p, is supposed to be unity. Therefore, the matrix elements exhibit the following relations in the symmetric system:

$$P_{11} = P_{22}, \tag{30}$$

$$P_{12} = P_{21}, \tag{31}$$

$$P_{11} + P_{21} = P_{22} + P_{12} = 1. \tag{32}$$

A similar matrix, which is referred to as the time-source matrix hereinafter, can be defined for the time source as follows:

$$\begin{pmatrix} Q_{11} & Q_{21} \\ Q_{12} & Q_{22} \end{pmatrix} \begin{pmatrix} T_1 \\ T_2 \end{pmatrix} = -\frac{1}{\alpha} \begin{pmatrix} T_1 \\ T_2 \end{pmatrix}, \tag{33}$$

where $Q_{ij} =$ the probability of a time source born in region *j* owing to one average time source starting in region *i*; $T_i =$ the time sources in region *i*. In this symmetric test problem, regions 1 and 2 for the time-source matrix are assigned to the left and right half parts, respectively, as shown in Fig. 4. The matrix elements and the eigenvalue exhibit the following relations in the symmetric system:

$$Q_{11} = Q_{22}, \tag{34}$$

$$Q_{12} = Q_{21}, \tag{35}$$

$$\alpha Q_{11} + \alpha Q_{12} = \alpha Q_{22} + \alpha Q_{21} = 1. \tag{36}$$

The matrix elements, P_{ij} and Q_{ij}, are shown in Tables 2 and 3, respectively. The degree of coupling between two regions can be represented by the nondiagonal elements, P_{12} or αQ_{12}. The fact that αQ_{12} is much larger than P_{12} can be understood by comparing Figs. 3 and 4. While the neutronic coupling of the fission sources between the two fissile slabs was interrupted by the thick isolator, time sources were produced even in the isolator, and neutrons passed frequently over the boundary between two regions, thereby causing αQ_{12} to be much larger than P_{12}.

[Fig. 4][Table 2][Table 3]

The time-source matrix elements were calculated in the same manner as the fission matrix in terms of the source regions. That is, the time source probability between two *fuel* slabs were calculated and they are listed in Table 4, where $\alpha Q_{F1\to F2}$, for example, denotes the probability of a time source born in the fuel slab 2 owing to one average time source starting in the fuel slab 1. $\alpha Q_{F1\to F2}$ and $\alpha Q_{F2\to F1}$ are almost half of $\alpha Q_{F1\to F1}$ and $\alpha Q_{F2\to F2}$. Thus, the time sources are still strongly coupled between two fuel slabs even though the fuel slabs are separated by the thick light water isolator.

[Table 4]

The α-eigenvalue calculations were performed using the k–α and time-source methods using the in-house research-purpose code. The calculations using the k–α method were

performed in 200 inactive generations and 10,000 active generations with 50,000 histories per generation. The calculations using the time-source method were performed in 10 inactive cycles and 800 active cycles with 20,000 histories per cycle. The first higher-order α-eigenvalues, α_1 were obtained using the method proposed by Booth (2003), Yamamoto (2009), and Yamamoto (2011). With the same method, the first higher-order eigenvalues of k_p (i.e., $k_{p,1}$) were obtained; $k_{p,1}$ is the first higher-order eigenvalue of Eq. (1) with a fixed fundamental mode α-eigenvalues, α_0. The eigenvalues are shown in Table 5. Using these eigenvalues, the dominance ratios of the k–α and the time-source methods are, respectively,

$$\rho_f = k_{p,1} = 0.99270 \pm 0.00003, \tag{37}$$

$$\rho_t = \frac{\alpha_0}{\alpha_1} = 0.329 \pm 0.001. \tag{38}$$

[Table 5]

The fundamental and first higher-order mode fission source distributions are shown in Fig. 5, and those of the time source are shown in Fig. 6. Fig. 5 shows that the fission-source distribution of the first-order higher mode is almost identical to that of the fundamental mode, which typically occurs in a loosely coupled system. In such a situation, $k_{p,1}$ can be approximated by the second eigenvalue of the fission matrix, Eq. (29), as follows:

$$k_{p,1} \approx \frac{P_{11} + P_{22} - \sqrt{(P_{11} + P_{22})^2 - 4P_{11}P_{22} + 4P_{12}P_{21}}}{2} = 0.99270, \tag{39}$$

which precisely agrees with ρ_f by Eq. (37). Meanwhile, as shown in Fig. 6, the fundamental mode time-source distribution is different from the first higher-order mode distribution, especially in the isolator. The first higher-order α-eigenvalue, α_1 is inaccurately approximated by the second eigenvalue of the time source matrix, Eq. (33), as follows:

$$\frac{-2}{Q_{11} + Q_{22} - \sqrt{(Q_{11} + Q_{22})^2 - 4Q_{11}Q_{22} + 4Q_{12}Q_{21}}} = -346\ \mathrm{s}^{-1}, \tag{40}$$

which is significantly overestimated compared with α_1 ($-309.2\ \mathrm{s}^{-1}$) in Table 5.

[Fig. 5][Fig. 6]

The performances of the source convergence are compared between the k–α and time-source methods. In Fig. 7, the ratio of the fission sources in both slabs, S_1/S_2, is plotted as

a function of generation when the initial source was uniformly distributed in slab 2 only. Approximately 400 generations were required for the fission source ratio to reach unity without using the Wielandt method ("ke = ∞" in Fig. 7). The ratios where the Wielandt method was applied are plotted in Fig. 7. Convergence was attained in fewer cycles as k_e decreased toward unity. Fig. 8 shows the relative CPU time per fission source and the relative figure of merit (FOM) as a function of k_e. The FOM is defined as the inverse of the product of the total CPU time and the square of the standard deviation of the α-eigenvalue. Whereas the CPU time per fission source decreases with k_e, the FOM increases with k_e. Although the Wielandt method improves the fission source convergence, the computational efficiency is not always improved in terms of the FOM, which has been reported previously (e.g., Yamamoto and Miyoshi., 2004).

[Fig. 7][Fig. 8]

Similarly, the ratios of the time source, T_1/T_2, are plotted in Fig. 9 when the initial time sources were allocated in the right-half region only. Without the Wielandt method ("αe = 0" in Fig. 9), the time-source method required only three cycles for the ratio to reach unity. This fast convergence can be attributed to the low dominance ratio or the large nondiagonal elements of the time-source matrix. However, because the fission chain per source is long with α_e =0, negative values were used for α_e to reduce the computation time per time source. The ratios, T_1/T_2, with some negative values of α_e are plotted in Fig. 9. The figure shows that the source convergence decelerates with the increase in α_e owing to the dominance ratio that is higher than that with $\alpha_e = 0$. Fig. 10 shows the relative CPU time per time source and the relative FOM of the α-eigenvalue as a function of α_e. Whereas the CPU time per time source decreases with the increase in α_e, the FOM is almost constant regardless of α_e. For example, when $\alpha_e =$ 500 s^{-1}, the source convergence is reached after 10 cycles and the FOM is almost the same as that with $\alpha_e = 0$, and the CPU time per time source is one fifth. A shorter computation time per source implies a shorter fission chain, which reduces the data storage for the time-source bank. Therefore, the use of an appropriate positive α_e is desirable provided that the source convergence and FOM remain satisfactory.

[Fig. 9][Fig. 10]

5.3 Convergence of time-source method above prompt criticality

The second example addresses a system slightly above the prompt criticality where $k_{eff,p} \approx 1.006$ and the fundamental mode α-eigenvalue $\alpha_0 \approx 167$ s^{-1}. The slab thickness W shown in Fig. 3 is 16.8 cm. A situation where the calculated $k_{eff,p}$ slightly exceeded unity despite the system being below the prompt criticality could occur owing to the biases in the calculation method. The eigenvalues obtained using the k–α method are shown in Table 6. In this system, the time-source method cannot be used without the Wielandt method. According to Eq. (24), α_e must be selected to be larger than α_0. Table 7 shows the α_0, dominance ratio, relative CPU time per time source, and relative FOM for $\alpha_e = 500$, 1000, and 2000 s^{-1}. The FOMs were almost constant regardless of α_e. The numerical tests in this section exemplifies that the Wielandt method enables the time-source method to be applied to super prompt critical systems.

[Table 6] [Table 7]

Besides the system slightly above the prompt criticality in this example, the time source method can be made available for a super critical system having a much higher k_{eff} if α_e is selected to be larger than α_0.

5.4 Convergence of α-eigenvalue in a deeply subcritical system

The two numerical tests above address a nearly prompt critical system. This section presents a different source convergence in a deeply subcritical system, where W = 7.0 cm, $k_{eff,p} \approx 0.611$, and $\alpha_0 \approx -5630$ s^{-1}. Owing to this large $|\alpha_0|$, the particles' weights increase significantly according to Eq. (5) while they travel in the isolator. This effect intensifies the neutronic coupling between the two slabs, compared with the k_{eff}-eigenvalue calculation. Fig. 11 compares the fission-source distributions calculated by the k_{eff}-eigenvalue calculation and k–α method. The fission-source distributions by the two methods are clearly different. The fission-source distribution of the k–α calculation shift toward the interface between the fuel and the isolator, which is due to the larger α eigenvalue. Table 8 shows the α_0, α_1, and $k_{p,1}$ values. Table 9 shows the dominance ratios of the k–α method, time-source method, and k_{eff}-eigenvalue

mode. The dominance ratio of the k–α method, $k_{p,1}$ is much smaller than unity, as predicted in the simple model in Section 3, whereas it is close to unity in the nearly prompt critical system, as shown in Tables 5 and 6. Meanwhile, the dominance ratio of the k_{eff}-eigenvalue mode, $k_{eff,p,1}/k_{eff,p}$ is still nearly unity, where $k_{eff,p,1}$ is the first higher-order eigenvalue of the prompt multiplication factor. The dominance ratio of the time-source method is much smaller than unity, but it is much larger than that in the nearly prompt critical system in Section 5.2, which is consistent with the result in Section 3. In Fig. 12, the ratios of the fission sources in both slabs, S_1/S_2 are plotted as a function of generation when the initial source was uniformly distributed in slab 2 only. The ratio of the time sources, T_1/T_2 is also plotted in the same figure. The convergence of the k–α method is much faster than that of the k_{eff}-eigenvalue mode calculation, and it is almost equivalent to that of the time-source method.

[Fig. 11][Fig. 12][Table 8][Table 9]

6. Conclusions

Issues regarding the source convergence of the k–α and time-source methods for α-eigenvalue calculations were discussed herein. The stability of time-source convergence is dominated by the ratio of the fundamental mode α-eigenvalue to the first higher-order α-eigenvalue, which is much smaller than the dominance ratio of the k–α method except for deeply subcritical systems. The convergence of the time-source method is primarily stable, especially in nearly critical systems.

However, the time-source method requires a longer computation time per source in nearly critical systems owing to the long-lasting fission chain. The Wielandt method is introduced herein to reduce the computation time of the time-source method and to increase the dominance ratio instead of decreasing it. This usage of the Wielandt method is contrary to the ordinary application of the Wielandt method, where it improves the fission source convergence in a k_{eff}-eigenvalue calculation by decreasing the dominance ratio. The adverse effect on the time-source convergence owing to the increase in the dominance ratio is limited because the dominance ratio of the time-source method is inherently low except in deeply subcritical systems. The time-source method cannot be applied to super prompt critical systems owing to the

endlessly continuing fission chain. However, the time source method becomes applicable to super prompt critical systems by introducing the Wielandt method.

In a deeply subcritical system, the dominance ratio of the k–α method is lower than that of the k_{eff}-eigenvalue mode calculation. The large α-eigenvalue in a deeply subcritical system enhances the neutronic coupling in the k–α method even in loosely coupled systems. Hence, the fission-source convergence of the k–α method becomes more stable in a deeply subcritical system, whereas the dominance ratio of the time-source method becomes larger with increasing depth of the subcriticality.

References

Booth, T.E., 2003. Computing the higher k-eigenfunctions by Monte Carlo power iteration: a conjecture. Nucl. Sci. Eng. 143, 291–300.

Brockway, D., Soran, P., Whalen, P., 1985. Monte Carlo α calculation, Tech. Rep. LA-UR-85-1224, Los Alamos National Laboratory.

Brown, F.B., 2011. "K-effective of the world" and other concerns for Monte Carlo eigenvalue calculations. Prog. Nucl. Sci. Technol. 2, 738–742.

Carney, S., Brown, F., Kiedrowski, B., Martin, W., 2014. Theory and applications of the fission matrix method for continuous-energy Monte Carlo. Ann. Nucl. Energy 73, 423–431.

Dufek, J., Gudowski, W., 2009. Stability and convergence problems of the Monte Carlo fission matrix acceleration methods. Ann. Nucl. Energy 36, 1648–1651.

Dufek, J., Holst, G., 2016. Correlation errors in the Monte Carlo fission source and the fission matrix fundamental-mode eigenvector. Ann. Nucl. Energy 94, 415–421.

Josey, C., Brown, F.B., 2018. A new Monte Carlo alpha-eigenvalue estimator with delayed neutrons. Trans. Am. Nucl. Soc. 118, 903–906.

Josey, C., Brown, F.B., 2019. Stabilizing the k-alpha algorithm in very subcritical regimes. Int. Conf. Math. Comput. Methods Applied to Nucl. Sc. Eng., 948–956.

Kiedrowski, B.C., 2014. Comparison of iterative time-eigenvalue methods with discrete

ordinates and Monte Carlo, Trans. Am. Nucl. Soc. 110, 203–206.

Nauchi, Y., 2014. Attempt to estimate reactor period by natural mode eigenvalue calculation. In: Proceedings of SNA+MC 2013, Paris, France.

Nauchi, Y., 2019. Estimation of time-dependent neutron transport from point source based on Monte Carlo power iteration. J. Nucl. Sci. Technol. 56, 996–1005.

Pan, L., Wang, R., Jiang, S., 2015. Monte Carlo fission matrix acceleration method with limited inner iteration. Nucl. Sci. Eng. 180, 199–208.

Shim, H.J., Kim, C.H., 2009. Tally efficiency analysis for Monte Carlo Wielandt method. Ann. Nucl. Energy 36, 1694-1701.

Shim, H. J., Jeong, B. K., Kang, S. M., Kim, C. H., 2014. Monte Carlo alpha iteration algorithm for a prompt neutron decay constant calculation. Trans. Am. Nucl. Soc. 111, 725–726.

Shim, H. J., Jang, S. H., Kang, S. M., 2015. Monte Carlo alpha iteration algorithm for a subcritical system analysis. Sci. Technol. Nucl. Installations 2015, Article ID 859242.

Ueki, T., 2012. Monte Carlo criticality calculation under extreme condition. J. Nucl. Sci. Technol. 49, 1134–1143.

Vitali, V., Chevallier, F. Jinaphanh, A., Blaise, P., Zoia, A., 2020. Spectral analysis by direct and adjoint Monte Carlo methods. Ann. Nucl. Energy 137, 107033.

Wachspress, E.L., 1966. Iterative Solution of Elliptic Systems and Applications to the Neutron Diffusion Equation of Reactor Physics, Prentice-Hall, Englewood Cliffs.

Whitesides, G.E., 1971. A difficulty in computing the k-effective of the world. Trans. Am. Nucl. Soc. 14, 680.

Woodcock, E. R., 1965. Techniques used in the GEM code for Monte Carlo neutronics calculations in reactors and other systems of complex geometry, Argonne National Laboratory, ANL-7050.

Yamamoto, T., Nakamura, T., Miyoshi, Y., 2000. Fission source convergence of Monte Carlo criticality calculations in weakly coupled fissile arrays. J. Nucl. Sci. Technol. 37, 41–52.

Yamamoto, T., Miyoshi, Y., 2003. An algorithm of α- and γ-mode eigenvalue calculations by

Monte Carlo method. Proc. 7th Int. Conf. on Nuclear Criticality Safety (ICNC '03), JAERI-Conf 2003-019, Japan Atomic Energy Research Institute, Tokai, Japan, October 2003.

Yamamoto, T., Miyoshi, Y., 2004. Reliable method for fission source convergence of Monte Carlo criticality calculation with Wielandt's method. J. Nucl. Sci. Technol. 41(2), 99–107.

Yamamoto, T. 2009. Convergence of the second eigenfunction in Monte Carlo power iteration. Ann. Nucl. Energy 36, 7–14.

Yamamoto, T., 2011. Higher order α mode eigenvalue calculation by Monte Carlo power iteration. Prog. Nucl. Sci. Technol. 2, 826–835.

Yamamoto, T., Sakamoto, H., 2019a. A Monte Carlo technique for sensitivity analysis of alpha-eigenvalue with the differential operator sampling method. Ann. Nucl. Energy 127, 178–187.

Yamamoto, T., Sakamoto, H., 2019b. Two-step Monte Carlo sensitivity analysis of alpha- and gamma-eigenvalues with the differential operator sampling method. Ann. Nucl. Energy 133, 100–109.

Zoia, A., Brun, E., Malvagi, F., 2014. Alpha eigenvalue calculations with TRIPOLI-4. Ann. Nucl. Energy 63, 276–284.

Zoia, A. Brun, E., Damian, F., Malvagi, F., 2015. Monte Carlo methods for reactor period calculations. Ann. Nucl. Energy 75, 627–634.

List of figures

Figure

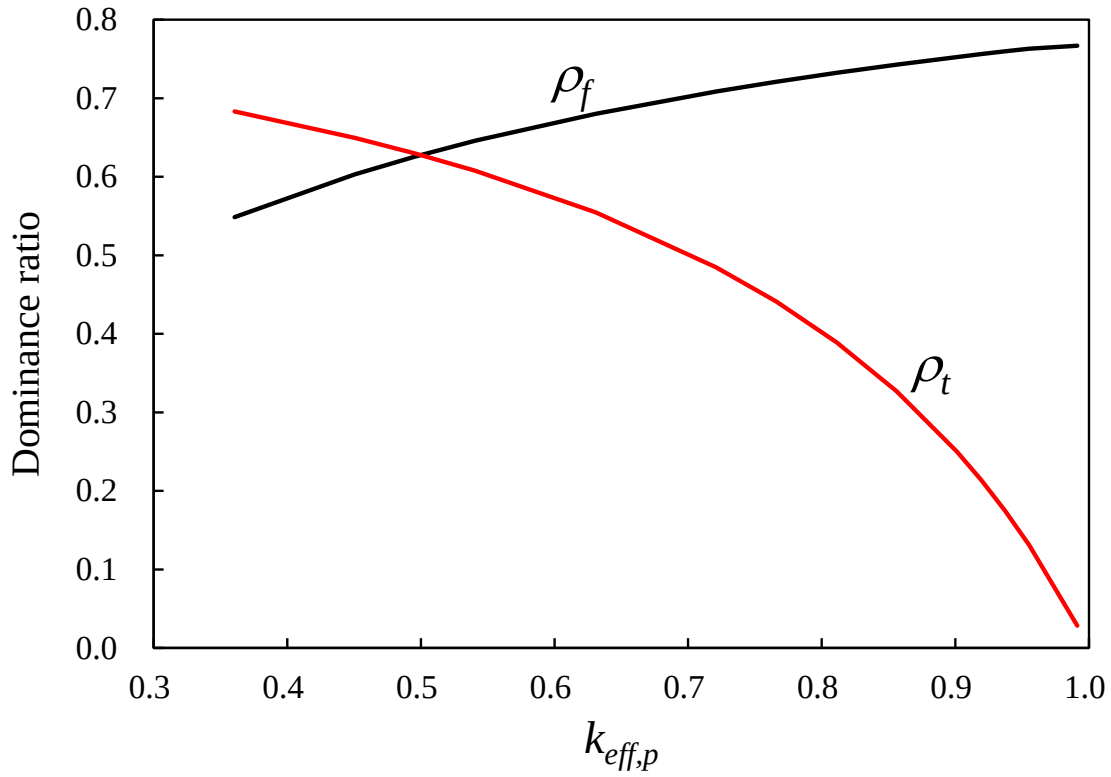

Fig. 1 Dominance ratios ρ_f of the k–α method and ρ_t of the time-source method as a function of $k_{eff,p}$.

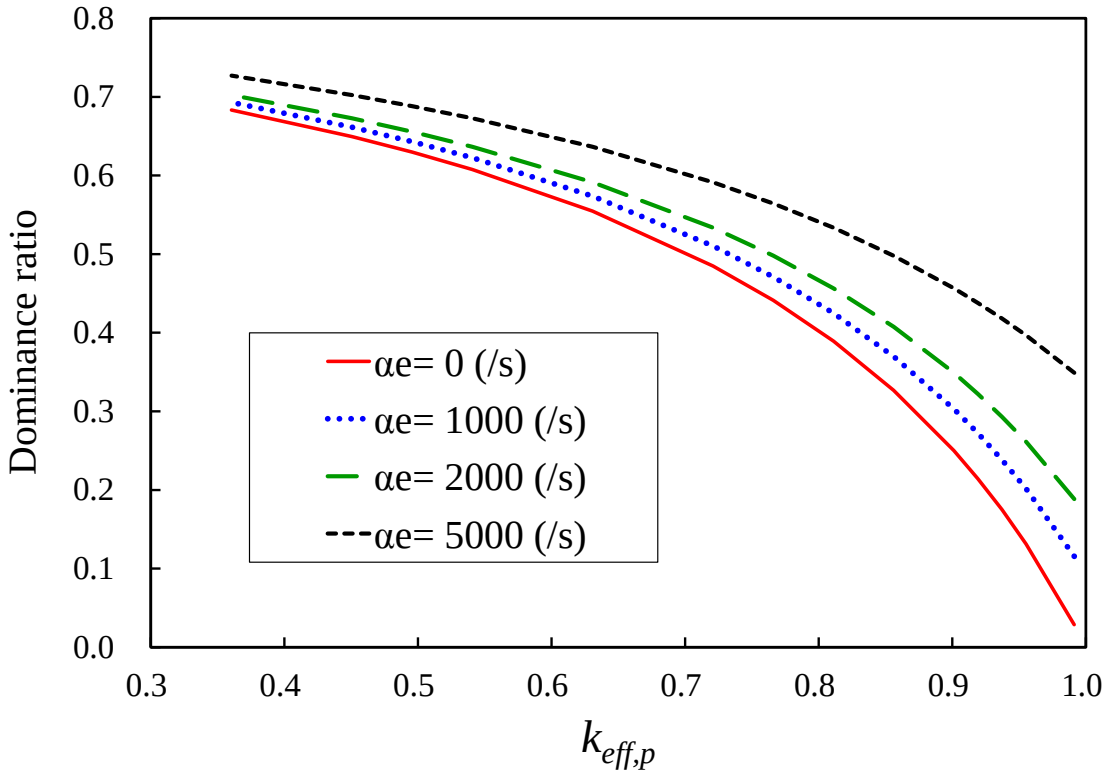

Fig. 2 ρ_t as a function of $k_{eff,p}$ for several α_e.

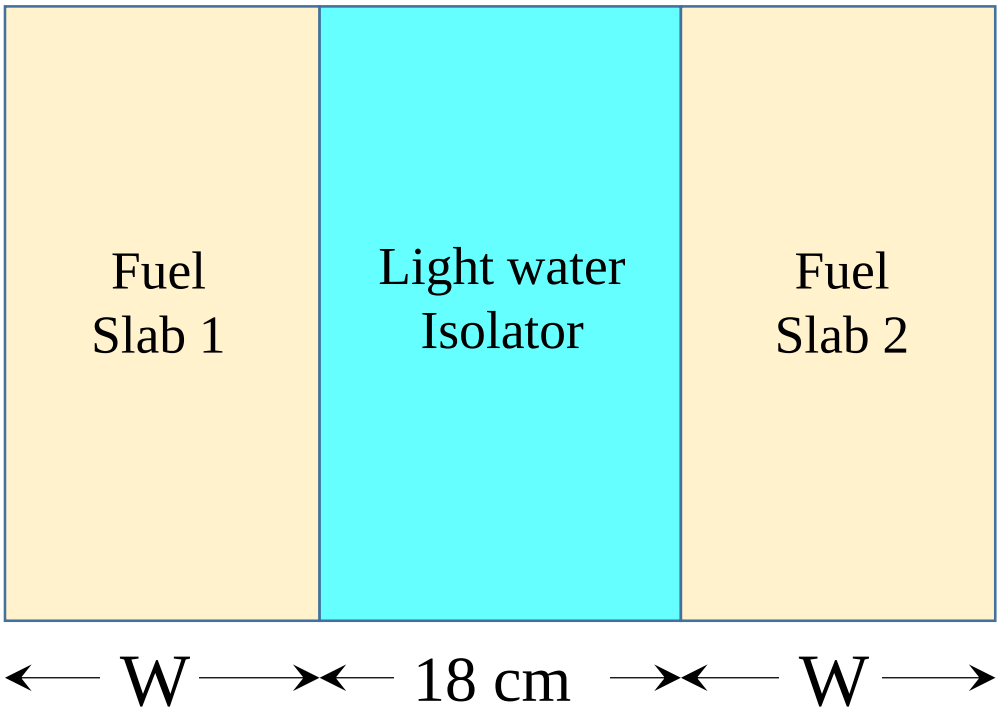

Fig. 3 One-dimensional two-slab array system for the k–α method.

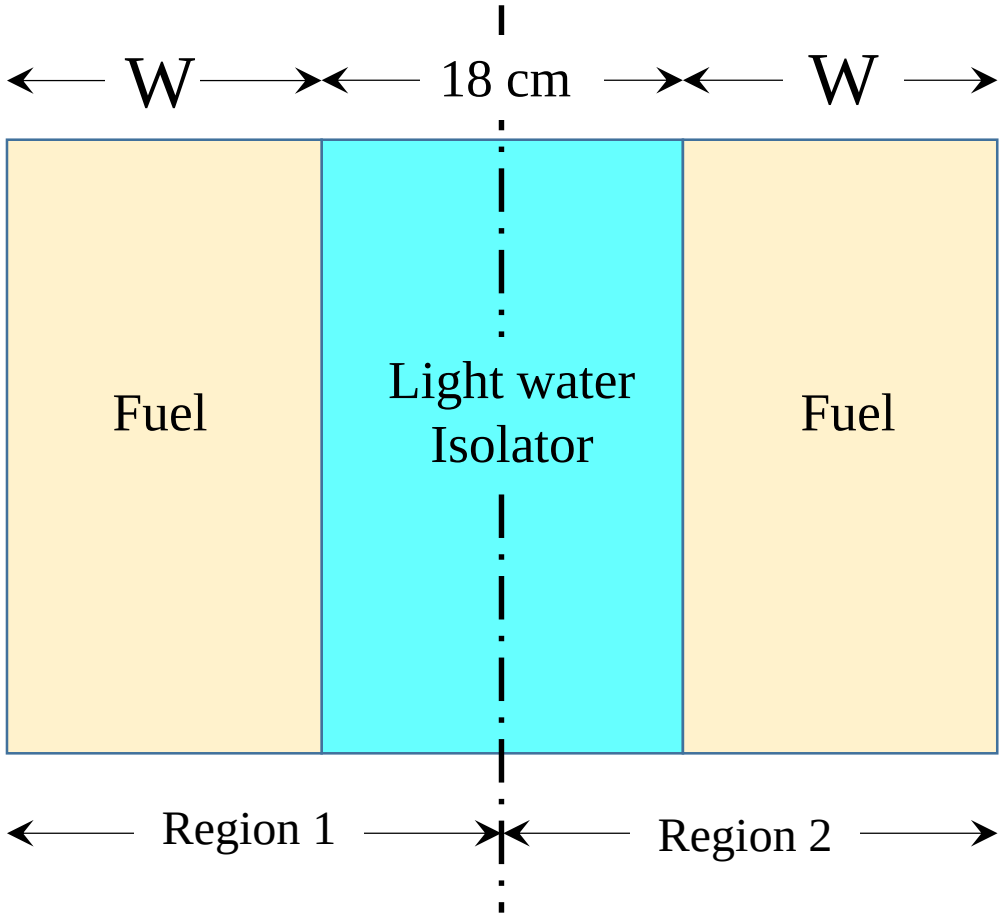

Fig. 4 One-dimensional two-slab array system for the time-source method.

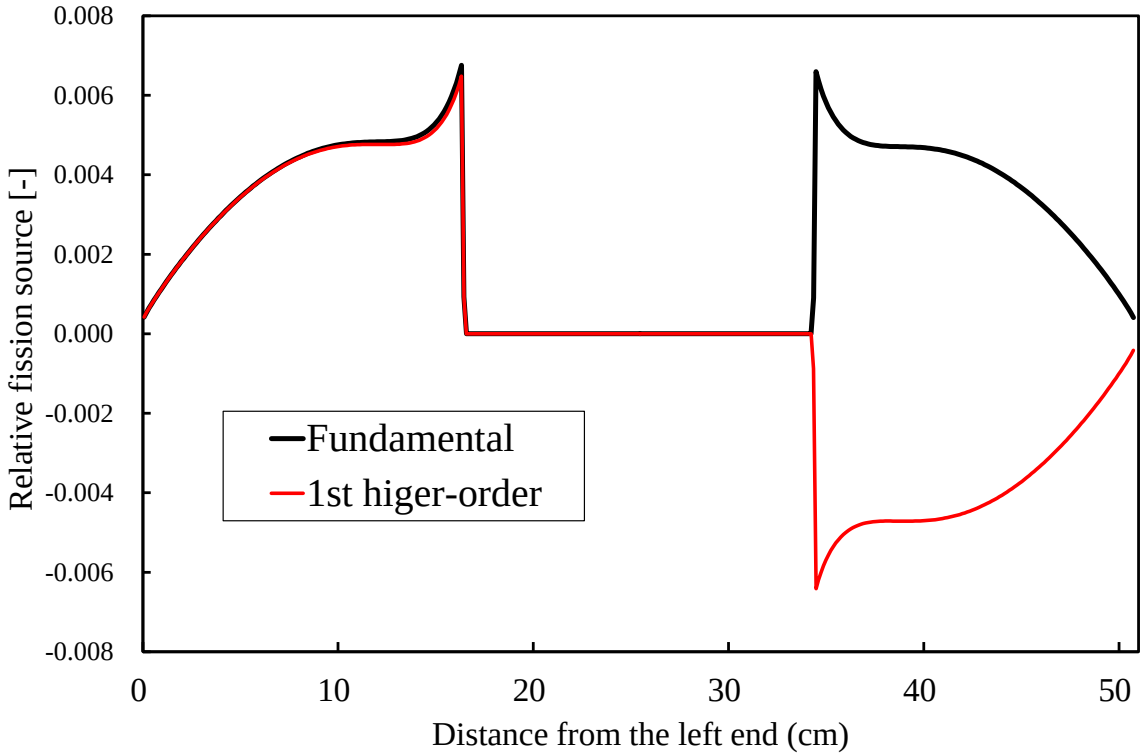

Fig. 5 Fission-source distributions of the fundamental and first higher-order modes.

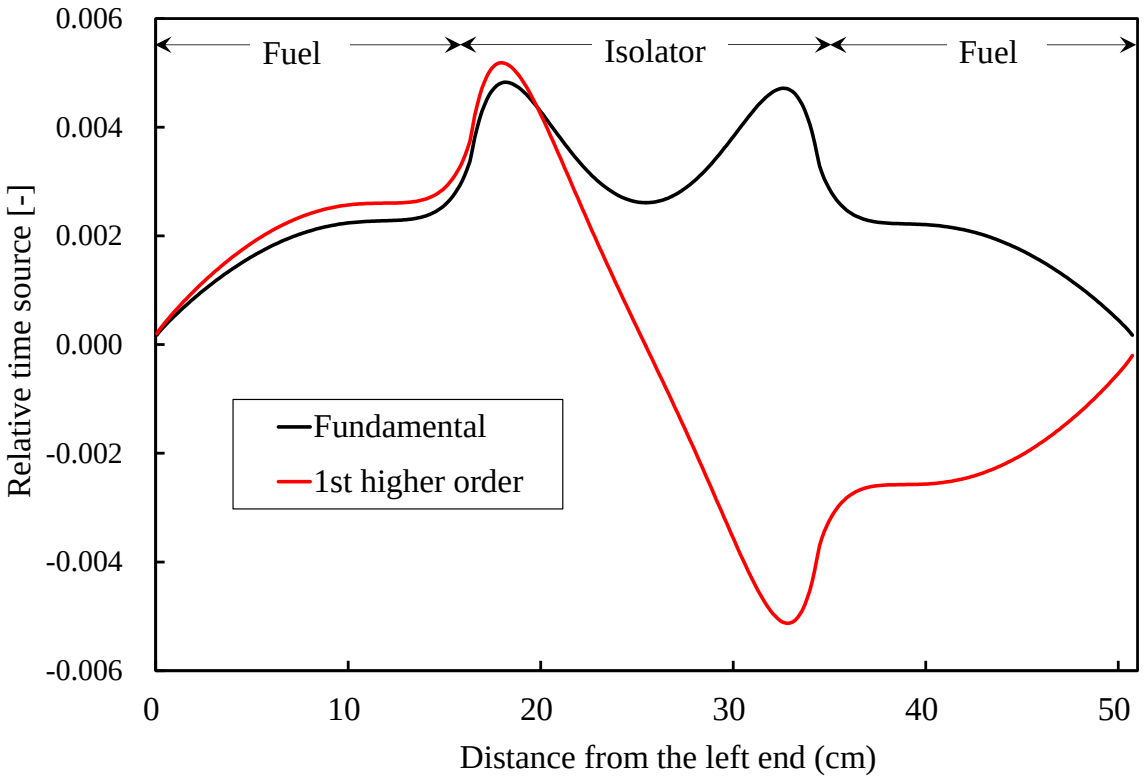

Fig. 6 Time-source distributions of the fundamental and first higher-order modes.

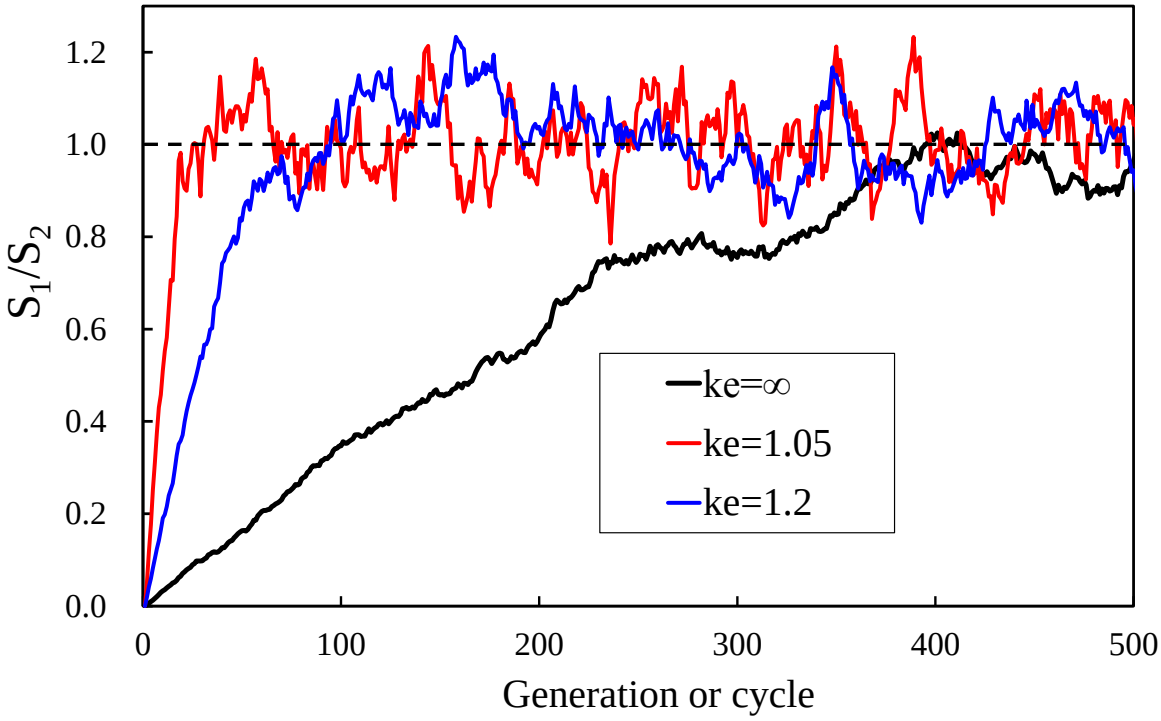

Fig. 7 Ratios of the fission sources in both slabs for k_e = 1.05, 1.2, and ∞.

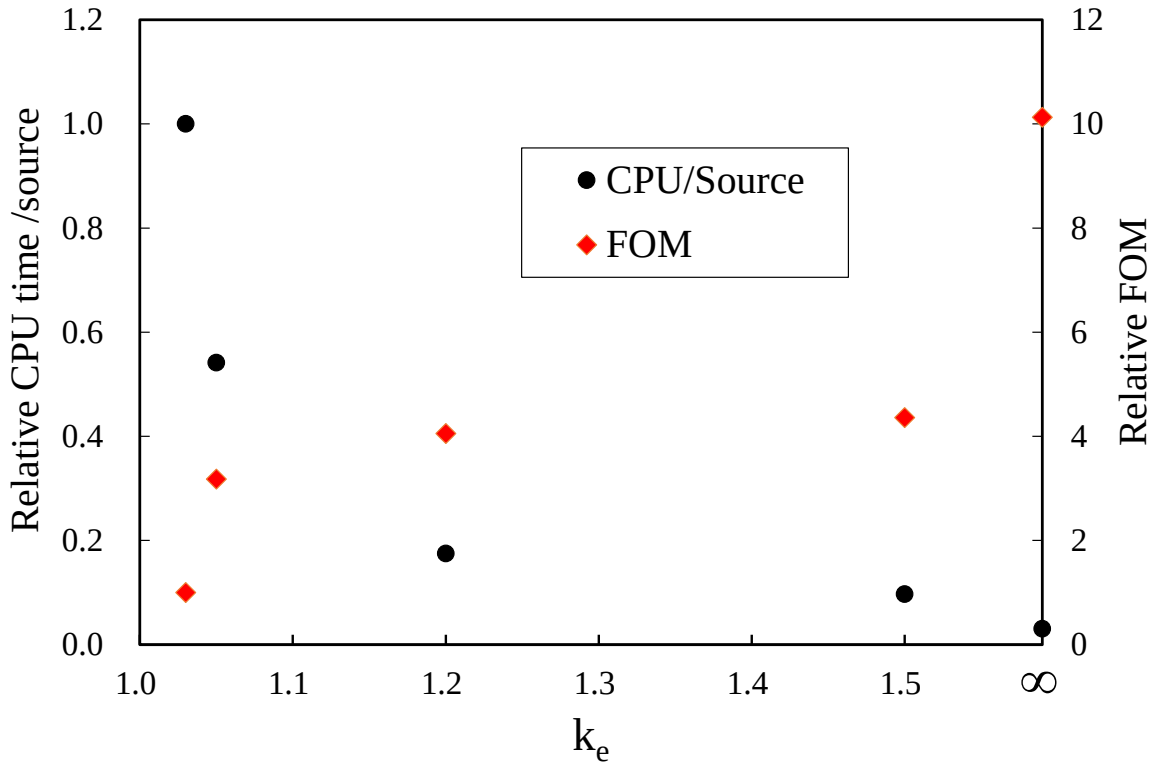

Fig. 8 Relative CPU time per source and relative FOM as a function of k_e.

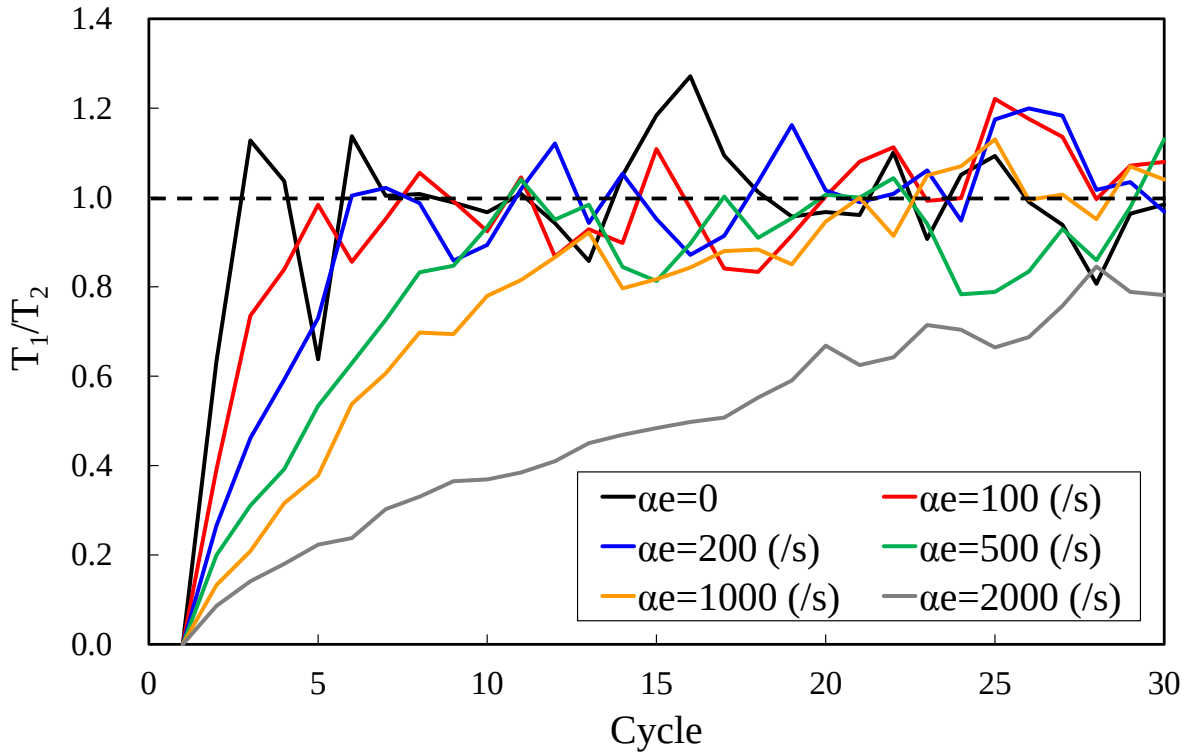

Fig. 9 Ratios of the time sources in both regions for α_e =0, 100, 200, 500, 1000, and 2000 s^{-1}.

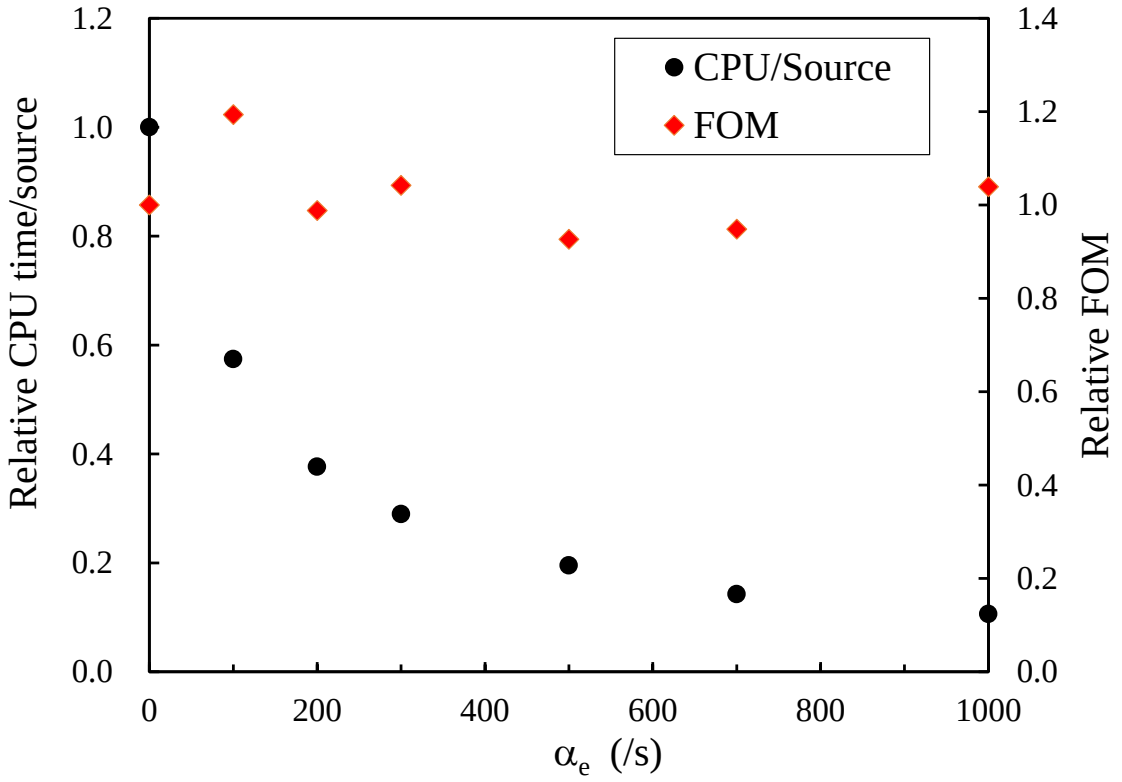

Fig. 10 Relative CPU time per source and relative FOM as a function of α_e.

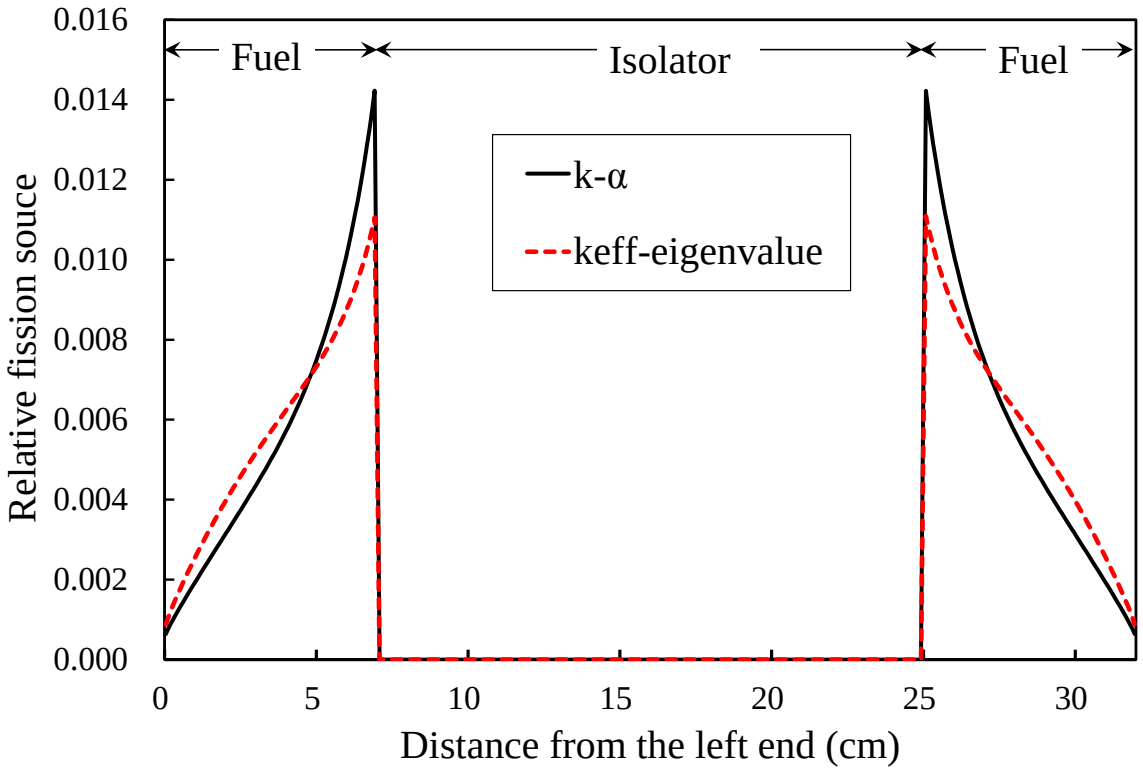

Fig. 11 Fission-source distributions of α-eigenvalue method and k_{eff}-eigenvalue mode in the deeply subcritical system.

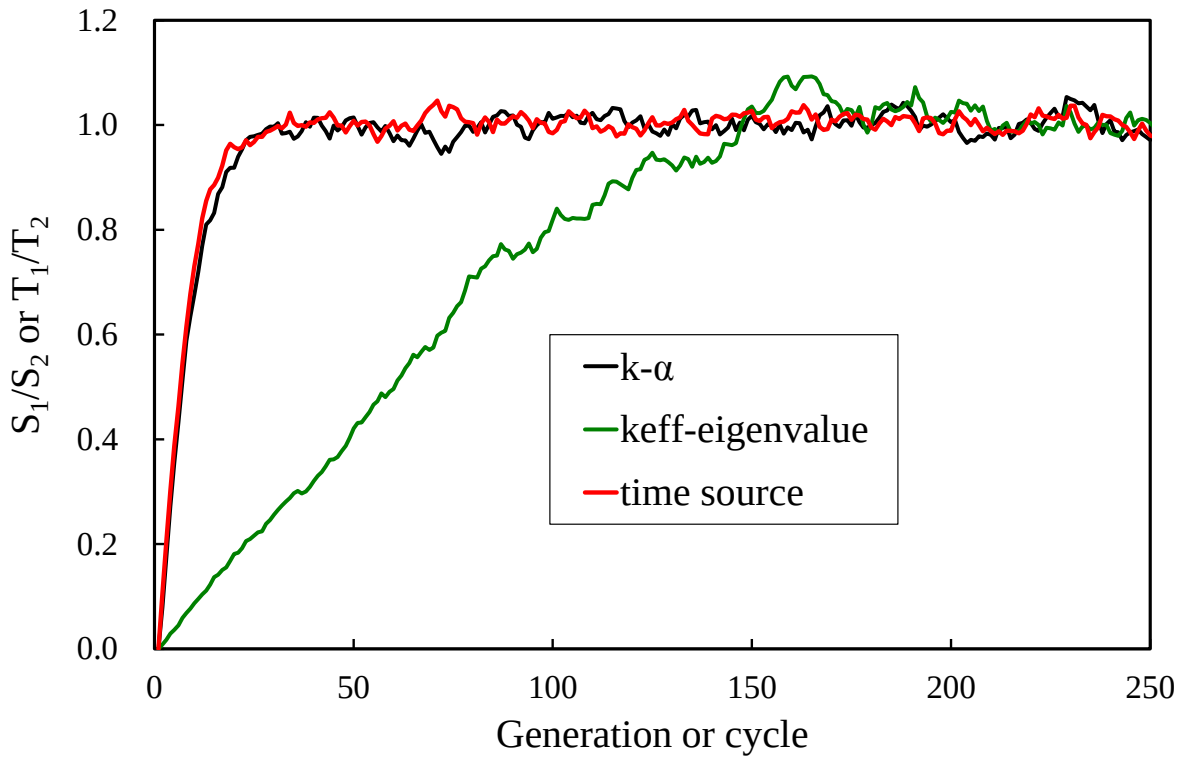

Fig. 12 Fission source ratios of α-eigenvalue and k_{eff}-eigenvalue modes and time-source ratio in the deeply subcritical system.

Table

Table 1 Three-group constants for UO_2 fuel rod array and light water

		UO_2 fuel rod array	Light water
Total cross section (cm^{-1})	Σ_{t1}	0.29829	0.33207
	Σ_{t2}	0.83334	1.1265
	Σ_{t3}	1.6389	2.7812
Fission cross section (cm^{-1})	Σ_{f1}	0.0030586	–
	Σ_{f2}	0.0021579	–
	Σ_{f3}	0.056928	–
Absorption cross section (cm^{-1})	Σ_{a1}	0.003385	0.00030500
	Σ_{a2}	0.011895	0.00036990
	Σ_{a3}	0.086180	0.0182500
Group transfer cross section (cm^{-1})	$\Sigma_s^{1\to2}$	0.073843	0.10464
	$\Sigma_s^{1\to3}$	0.0	0.0
	$\Sigma_s^{2\to3}$	0.043803	0.097961
Neutrons per fission	ν_p	2.4	–
Fission spectrum	χ_{p1}	0.878198	–
	χ_{p2}	0.121802	–
	χ_{p3}	0	–
Neutron velocity (cm/s)	v_1	1.66743×10^9	
	v_2	1.73734×10^7	
	v_3	3.46850×10^5	

Table 2 Elements of the fission matrix for $W = 16.4$ cm

P_{11}	0.99638 ± 0.00004	P_{21}	0.003646 ± 0.000004
P_{12}	0.003645 ± 0.000004	P_{22}	0.99633 ± 0.00004

Table 3 Elements of the time source matrix for $W = 16.4$ cm

αQ_{11}	0.64944 ± 0.0041	αQ_{21}	0.35278 ± 0.0034
αQ_{12}	0.35441 ± 0.0034	αQ_{22}	0.64479 ± 0.0041

Table 4 Elements of the time source matrix for $W = 16.4$ cm

$\alpha Q_{F1\to F1}$	0.53266 ± 0.0045	$\alpha Q_{F2\to F1}$	0.26255 ± 0.0038
$\alpha Q_{F1\to F2}$	0.26164 ± 0.0037	$\alpha Q_{F2\to F2}$	0.53801 ± 0.0048

Table 5 Fundamental and first higher-order mode eigenvalues for $W = 16.4$ cm

	α_0 (s^{-1})	α_1 (s^{-1})	$k_{p,1}$
k-α	−101.6 ± 0.3	−309.2 ± 0.2	0.99270 ± 0.00003
Time source	−103.8 ± 0.6	—	—

Table 6 Fundamental and first higher-order mode eigenvalues by the k-α method for $W = 16.8$ cm

	α_0 (s^{-1})	α_1 (s^{-1})	$k_{p,1}$	$k_{eff,p}$ *
k-α	166.8 ± 0.3	−280.5 ± 0.2	0.99330 ± 0.00004	1.00597 ± 0.00003

*Eigenvalue k_p in Eq. (1) with $\alpha = 0$.

Table 7 Results of the time source method for $W = 16.8$ cm

α_e (s^{-1})	α_0 (s^{-1})	Dominance ratio	Relative CPU time/source	Relative FOM
500	165.5 ± 1.3	0.427	1.00	1.00
1000	164.8 ± 1.8	0.651	0.40	1.02
2000	166.3 ± 1.3	0.804	0.18	1.01

Table 8 Fundamental and first higher-order mode eigenvalues for $W = 7$ cm

	α_0 (s^{-1})	α_1 (s^{-1})	$k_{p,1}$
k-α	−5630.6 ± 0.1	−6910.7 ± 0.7	0.85706 ± 0.00004
Time source	−5631.0 ± 0.8	—	—

Table 9 Dominance ratios by the three methods for $W = 7$ cm

	Dominance ratio	Remark
k-α	0.857	$= k_{p,1}$
Time source	0.814	$= \alpha_0/\alpha_1$
k_{eff}-eigenvalue	0.981	$= k_{eff,p,1}/k_{eff,p}$

$k_{eff,p}$= 0.61122 ± 0.00003

$k_{eff,p,1}$= 0.59935 ± 0.00003

Declaration of interest statement

The authors declare no conflicts of interest associated with this manuscript.

CRediT authorship contribution statement

Toshihiro Yamamoto: Supervision, Methodology, Conceptualization, Investigation, Writing - original draft. **Hiroki Sakamoto**: Software, Validation, Formal analysis, Data curation, Writing - review & editing.